Structure and mechanisms underlying ion transport in ternary polymer electrolytes containing ionic liquids

Santosh Mogurampelly and Venkat Ganesan

Citation: The Journal of Chemical Physics **146**, 074902 (2017); doi: 10.1063/1.4976131
View online: http://dx.doi.org/10.1063/1.4976131
View Table of Contents: http://aip.scitation.org/toc/jcp/146/7
Published by the American Institute of Physics

Structure and mechanisms underlying ion transport in ternary polymer electrolytes containing ionic liquids

Santosh Mogurampelly[1] and Venkat Ganesan[2,a)]
[1]*Department of Chemical Engineering, University of Texas at Austin, Austin, Texas 78712, USA*
[2]*Department of Chemical Engineering and Institute for Computational and Engineering Sciences, University of Texas at Austin, Austin, Texas 78712, USA*

(Received 8 November 2016; accepted 26 January 2017; published online 17 February 2017)

We use all atom molecular dynamics simulations to investigate the influence of 1-butyl-3-methylimidazolium hexafluorophosphate ($BMIMPF_6$) ionic liquid on the structure and transport properties of poly(ethylene oxide) (PEO) polymer electrolytes doped with $LiPF_6$ salt. We observe enhanced diffusivities of the Li^+, PF_6^-, and $BMIM^+$ ions with increasing loading of the ionic liquid. Interplay between the different ion-ion and ion-polymer interactions is seen to lead to a destabilization of the Li–PF_6 coordination and increase in the strength of association between the Li^+ cations and the polymer backbone. As a consequence, the polymer segmental relaxation times are shown to be only moderately affected by the addition of ionic liquids. The ionic-liquid induced changes in the mobilities of Li^+ ions are seen to be correlated to polymer segmental relaxation times. However, the mobilities of $BMIM^+$ ions are seen to be more strongly correlated to the BMIM–PF_6 ion-pair relaxation times. *Published by AIP Publishing.* [http://dx.doi.org/10.1063/1.4976131]

I. INTRODUCTION

Recently, significant interest has arisen in ionic liquids (ILs) for a variety of applications such as gas storage, photovoltaics, heat transfer fluids, energy storage, and batteries.[1–3] Such an interest stems from the novel physical properties of ILs such as low vapor pressure, high thermal stability, and nonflammability. In particular, ILs possess excellent ionic conducting properties at ambient temperatures and are being explored for battery applications as an additive to polymer-salt binary electrolytes which often possess requisite mechanical strengths but lack the desired room temperature conductivities.[4–9] On one hand, introduction of ILs to such polymer electrolytes increases the number of inherent charge carriers and thereby contributes to the conductivity of the electrolyte. Additionally, it is also believed that ILs act as plasticizers and accelerate the polymer dynamics and thereby increases the conductivity of the electrolyte.[10,11] Consistent with the latter hypothesis, experiments have reported[5,12–16] that the addition of ILs such as *N*-methyl-*N*-propylpyrrolidinium bis(trifluoromethanesulfonyl)imide ($PYR_{13}TFSI$) and 1-butyl-3-methylimidazolium hexafluorophosphate ($BMIMPF_6$) in binary poly(ethylene oxide) (PEO)-salt electrolytes results in increased ionic conductivity and wider electrochemical stability. In a different context, Li *et al.*[17] synthesized gel polymer electrolytes containing different loadings of $BMIMPF_6$. They also observed increased conductivity with increasing IL content and demonstrated a corresponding acceleration in polymer dynamics reflected in the decreased glass transition temperature.

Motivated by the above experimental interest, a number of computer simulation studies, especially atomistic molecular dynamics (MD) simulations, have examined the fundamental mechanisms underlying the physical properties of mixtures of polymers and ionic liquids. For instance, Yethiraj and co-workers[18] studied the conformational properties of isolated PEO chain in 1-butyl-3-methylimidazolium tetrafluoroborate (BMIM–BF_4) ionic liquid using atomistic simulations. They found that the BMIM–BF_4 acts as a good solvent for the polymer chain and leads to an expanded conformation of PEO. Recently, Raju *et al.*[19] used MD simulations to study the effect of alkyl chain length on the structure and dynamic properties of PEO dispersed with *N*-alkyl-*N*-methylpyrrolidinium TFSI (PEO-C_nMPyTFSI, n = 1, 3, 6, 9) electrolytes. They reported an increased ion-pairing in polymer-IL electrolyte and higher diffusivity of ions in the polymer-IL mixture compared to *pure* IL system. Heuer and co-workers[10,11] studied the properties of PEO-LiTFSI polymer-salt electrolytes with the addition of $PYR_{13}TFSI$ ionic liquid. They observed increased lithium ion mobilities, which they rationalized as a consequence of IL induced changes in polymer dynamics. In a series of articles, Costa *et al.*[20–22] reported the results of MD simulations of PEO mixed with ILs and, in some cases, with additional salt. Their studies characterized the equilibrium coordination behavior of the different atoms and the dynamical properties of such mixtures.

Despite the extensive amount of simulation studies in the context of mixtures of polymer and ILs, some unresolved issues remain.[10,11,22] Specifically, while computer simulations have elucidated the influence of ILs on the polymer segmental dynamics and ionic mobilities, there are far fewer studies which have analyzed the correlation between such characteristics and their IL loading dependencies. Moreover, while the influence of the ILs has been studied, there is much less information on the temperature dependence of the different mechanisms underlying the influence of ILs. The

a)venkat@che.utexas.edu

latter considerations are especially motivated by the fact that experiments have noted that introduction of ILs leads to larger relative increases in ionic conductivities at lower temperatures when compared to higher temperatures.[5,13] Finally, much of the simulation studies have concerned with TFSI based ILs and salts. There is less clarity on the universality of the mechanisms and the ion coordination behaviors in the context of blends based on other ILs and anions.

Motivated by the above issues, in this study we used atomistic computer simulations of ternary polymer-salt-IL mixtures of 1-butyl-3-methylimidazolium hexafluorophosphate ($BMIMPF_6$) ionic liquid with poly(ethylene oxide) polymer electrolytes doped with $LiPF_6$ to address the following questions:

- What is the influence of ILs on the coordination of the lithium ion with the anion and the polymer backbone?
- What are the influences of the loading of the IL and temperatures upon the ionic mobilities of the ternary electrolyte?
- What are the time scales/mechanisms underlying the transport properties of the cations and anions of the IL?

The organization of the rest of the paper is as follows: In Section II, we describe details of the interaction potentials, system setup, and different measures used to quantify our results. In Section III A, we present the results for ion association behavior including lithium ion coordination with anions and polymer, and $BMIM^+$ interaction with polymer segments. Sections IIIB and III C contain results for the ion mean squared displacements, ionic diffusivities, polymer, and ion-pair relaxation times. This is followed in Section III D by a discussion on the mechanisms underlying ionic mobilities in polymer-salt-IL electrolytes. In Section IV, we present a brief summary of our results.

II. SIMULATION DETAILS

A. Interaction potentials and force fields (FFs)

We used the following potential to describe the interactions in PEO–$LiPF_6$–$BMIMPF_6$ ternary electrolytes:

$$U(\boldsymbol{r}) = U^{\text{bonded}}(\boldsymbol{r}) + \sum_{i}^{N}\sum_{j>i}^{N} f_{ij}\left[4\epsilon\left[\left(\frac{\sigma_{ij}}{r_{ij}}\right)^{12} - \left(\frac{\sigma_{ij}}{r_{ij}}\right)^{6}\right] + \frac{q_i q_j e^2}{r_{ij}}\right], \quad (1)$$

where $U^{\text{bonded}}(\boldsymbol{r})$ refers to the bonded interactions and has contributions arising from all intramolecular bonds, angles, and torsions. The bond and angle interactions were modeled with harmonic potentials and the torsions were modeled with the optimized potentials for liquid simulations (OPLS) torsion potential. The non-bonded interactions $U_{\text{nb}}(r)$ included 12-6 Lennard-Jones potential and Coulomb potential with f_{ij} = 0.5 for 1-4 interactions which are bonded. The geometric combining rules $\epsilon_{ij} = \sqrt{\epsilon_{ii}\epsilon_{jj}}$ and $\sigma_{ij} = \sqrt{\sigma_{ii}\sigma_{jj}}$ were used to calculate interaction parameters for cross-terms in the non-bonded potential. Lennard-Jones interactions were truncated at 10 Å and tail corrections to the pressure and energy was included.

The force field (FF) parameters for PEO and IL were obtained from the optimized potentials for liquid simulations–all atom (OPLS-AA) FF set developed by Jorgensen[23] with improved intramolecular parameters from Acevedo.[24] In earlier studies, the OPLS-AA force fields have been widely used to simulate the properties of *pure* ILs and polymers.[18,25,26] While the OPLS-AA force fields have been found to reproduce accurately many of the structural properties in such systems,[24] the dynamic properties of *pure* ILs have been found to be underestimated due to the absence of polarization effects induced by ions. While recent work has suggested alternatives using fully polarizable force fields for ILs,[26–31] such an effort proves to be computationally expensive for studying polymer-IL mixtures. To overcome such issues, several researchers have proposed a scaling of the partial atomic charges, parametrized either based on *ab initio* quantum level calculations or empirically, for the force field parameters for the ionic species.[32–38] For instance, Maginn and co-workers[32,37,39] proposed a scaling of anionic and cationic charges and used such FFs to accurately estimate the shear viscosity and self-diffusion coefficient of ILs. Müller-Plathe and van Gunsteren[40] considered scaling of partial charges on the ions and successfully reproduced the experimental results for the ionic diffusivities.[26,39,41–45] Recently, Costa *et al.*[22] considered various FFs and observed that the use of reduced charges in the FFs yields results in better accordance with experiments.

Based on the success of the above studies,[33–35,43,44] in our present work we used a uniform scaling factor of 0.8 on the charges of cation and anion of the IL, similar to the procedure adapted in previous reports. To provide support for the adopted scaling factor, we performed a geometry optimization of single isolated IL pair using the density functional theory (DFT) method[46,47] with B3LYP/6-311** basis set.[48,49] From the fitting of electrostatic potential around the ionic pair, we obtained the net charge of the anion or cation to be 0.827 e, which is close to the factor of 0.8 we chose for our studies. Optimized geometry and the distribution of electrostatic potential around the $BMIMPF_6$ complex obtained from DFT calculations were shown in Figure 1. In addition to the scaling of charges on $BMIM^+$ and PF_6^- ions, we also reduce the partial atomic charge of Li^+ ions by a factor of 0.8 to ensure consistency with the reduced charge on the anions. For selected parameters, we also studied the transport properties using unscaled charges on the ions. We found that while the force field with full charges resulted in slower mobilities of ions, the qualitative trends were similar to those observed with the scaled charge force fields (the corresponding results are presented in Figure S1 of the supplementary material).

B. System setup

The initial configurations of binary electrolytes of *pure* IL and *pure* PEO systems were prepared using PACKMOL software.[50] For *pure* IL, 256 pairs of $BMIM^+$ cations and PF_6^- anions were randomly inserted in a simulation box corresponding to a low density. Similarly, pre-equilibrated configuration of a single poly(ethylene oxide) chain with the chemical structure of $H–[CH_2–O–CH_2]_{55}–H$ equivalent to a molecular weight of 2.425 kDa was solvated with an appropriate number of Li^+ and PF_6^- ions to obtain a desired salt concentration of

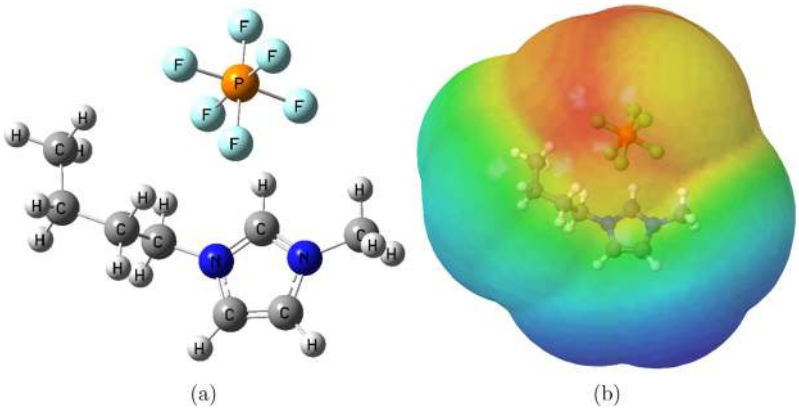

FIG. 1. (a) Optimized molecular structure of a single isolated $BMIMPF_6$ ion-pair and (b) the distribution of electrostatic potential around optimized ion-pair calculated using density functional theory (DFT) at B3LYP/6-311** theory level.[48,49] The value of the electrostatic potential is minimum in blue colored grids and maximum in red colored grids.

EO:Li = 15:1. Periodic boundary conditions were applied in all the three directions. To build the ternary electrolyte system at different loadings of IL, a sufficient number of ion-pairs were randomly distributed in the polymer-salt binary mixture. System details such as the number of ionic species at various loadings of the IL and corresponding equilibrium densities at different temperatures are provided in Table I.

The above initial configurations were subjected to an equilibration protocol described in our previous articles.[51,52] After equilibration, ternary electrolyte systems having different weight percentages of IL were simulated at different temperatures *viz.*, 450 K, 425 K, 400 K, 375 K and 350 K. Binary polymer-salt electrolyte systems were also simulated at 325 K and 300 K for comparison with the ternary system. All MD simulations were carried out using LAMMPS simulation package[53] at a constant number of particles, temperature, and pressure (NPT) ensemble. A 20 ns trajectory was obtained for each system for the analysis. For T = 425 K, we simulated up to 50 ns at all loadings of IL into polymer-salt mixture.

The trajectories obtained from atomistic MD simulations were of the order of 20-50 nanoseconds (ns) in duration. However, much longer trajectories are desired for studying ion diffusion properties in polymer matrices. To achieve this, we used the trajectory extending kinetic Monte Carlo (TEKMC) method to extend the trajectories proposed by Neyertz and Brown.[54] The idea behind TEKMC is to calculate the transition rate matrix for ions within the simulation box from MD trajectories and use them in a kinetic Monte Carlo scheme to evolve ionic species in time. Specifically, we map atomistic MD simulation box to a fictitious lattice framework with a grid size D_{grid} and analyze the input atomistic coordinates separated by time interval t_{input}. The centers of mass of PF_6^- and $BMIM^+$ ions were considered for the analysis and assume them to be point particles. Equilibrium MD trajectory was used to identify all possible transition events of penetrant particles (Li^+, PF_6^- and $BMIM^+$ ions) between penetrant cells (say, i and j) and calculate respective transition rate constants, $\{k_{ij}\}$, from cell i to cell j. The transition rates between different cells were averaged over the input atomistic simulation trajectory and are treated as constants during the KMC simulations. Rate constants calculated from equilibrium MD simulations were then used to evolve ions in time using Bortz-Kalos-Lebowitz (BKL) algorithm,[55] thus allowing us to obtain a long time evolution of ions.

The optimization of D_{grid} and t_{input} was achieved by matching the mean-squared displacement (MSD) for ions obtained from TEKMC with that of MD for short time scales at all temperatures and loadings of IL. The above procedure is repeated for each ionic species separately since they exhibit different diffusive characteristics and a separate optimization is required. With the optimization performed and transition rate matrix calculated, we extended atomistic trajectories for Li^+, PF_6^-, and $BMIM^+$ ions up to few microseconds (μs) in which regime the MSDs are found to exhibit a clear diffusive behavior.

C. Quantification measures

We used a variety of different static and dynamical measures to characterize our results and understand the mechanisms underlying ion transport in such ternary blends.

TABLE I. Simulation details of polymer-salt-IL ternary electrolyte with varying IL content and equilibrium densities obtained at various temperatures. Values in parentheses indicate the standard deviation to the density in units of 10^{-3} g/cc.

					ρ (g/cc)				
wt. %	#IL	#Li^+	#PF_6^-	#$BMIM^+$	350 K	375 K	400 K	425 K	450 K
0	0	73	73	0	1.184(6)	1.162(6)	1.140(7)	1.120(7)	1.097(7)
9	21	73	94	21	1.200(6)	1.179(6)	1.156(6)	1.134(7)	1.112(7)
17	42	73	115	42	1.199(5)	1.176(6)	1.154(6)	1.133(7)	1.111(7)
23	63	73	136	63	1.208(5)	1.182(6)	1.159(6)	1.138(6)	1.116(7)
29	84	73	157	84	1.210(5)	1.188(5)	1.164(6)	1.142(6)	1.120(7)
33	105	73	178	105	1.212(5)	1.190(5)	1.167(6)	1.145(6)	1.124(6)

Most of the measures adopted are common in the literature and have also been used in our earlier studies, and hence we provide only a brief description below.[51,56–58]

1. Radial distribution functions

The ion coordination features were characterized by calculating the radial distribution functions $g_{AB}(r)$ for different ion-ion and ion-polymer atomic pairs, where A, B represents particles of type A and B, respectively. The local environment around particles of type A is characterized in terms of the coordination number of particles of type B as

$$CN_B(r) = 4\pi\rho_B \int_0^r r^2 g_{AB}(r) dr, \tag{2}$$

where ρ_B is the number density of particles of type B.

2. Cluster size distribution functions

Earlier studies have suggested that there is a strong tendency for clustering of the cation-anion pairs in ILs.[59–62] To probe such features in our system, we employed a cluster analysis of the ion-ion and ion-polymer pairs using an approach suggested by Ottino and co-workers.[63] Briefly, ion-ion and Li^+–EO pairs in contact are identified to be "in-contact" when they are found to be within the distance corresponding to the first coordination shell of their radial distribution functions. Such pairs are used to build a connectivity matrix of different pairs of "associated" atoms. Such a connectivity matrix is then transformed to account for the indirect contact among the different ions and thereby identify the number of clusters of specific size s. Explicitly, we compute $N(s)$, the average fraction of particles of size s,[64–67]

$$N(s) = \left(s/N_p\right) n(s), \tag{3}$$

where N_p denotes the total number of particles and $n(s)$ represents the average number of the clusters.

3. Mean-squared displacements and diffusivity

The transport properties of both the cations and anions were probed by calculating the MSDs at various temperatures and weight percentages of the IL. The MSDs were then used to calculate the diffusion coefficient (D_α) of ionic species α using Einstein relation,

$$D_\alpha = \lim_{t\to\infty} \frac{1}{6t} \left\langle \left(\boldsymbol{R}_\alpha(t) - \boldsymbol{R}_\alpha(0)\right)^2 \right\rangle. \tag{4}$$

4. Polymer segmental dynamics

To probe the segmental dynamics of the PEO chains, we calculated the autocorrelation function of dihedral angle involving C–O–C–C atoms using[68,69]

$$C_{\phi\phi}(t) = \frac{\langle \cos\phi(t)\cos\phi(0)\rangle - \langle\cos\phi(0)\rangle^2}{\langle \cos\phi(0)\cos\phi(0)\rangle - \langle\cos\phi(0)\rangle^2}, \tag{5}$$

where $\phi(t)$ is the dihedral angle involving C–O–C–C atoms in PEO chain at time t. The results of $C_{\phi\phi}(t)$ were fitted to a Kohlrausch-Williams-Watts (KWW) stretched exponential function of the form, $\exp(-(t/t^*)^\beta)$ (where t^* and β are fitting parameters), and the mean relaxation time, τ of the polymer segments is evaluated as

$$\tau \equiv \langle\tau\rangle = \int_0^\infty \exp\left[-\left(\frac{t}{t^*}\right)^\beta\right] dt = t^*\Gamma\left(1+\frac{1}{\beta}\right) \tag{6}$$

where Γ denotes the Gamma function.

5. Normal mode analysis (NMA)

In addition to the dihedral angle relaxations, we also carried out a normal mode analysis (NMA) of the chain dynamics to provide an independent quantification of the polymer dynamics. For this purpose, the atomistic coordinates of PEO chain was converted to a bead-spring coarse-grained model wherein each CH_2–O–CH_2 monomer is represented as a single bead. Subsequently, we obtained the normal modes by explicitly diagonalizing the matrix of chain coordinates (relative to their center-of-mass) in our trajectories.[70] For a melt of unentangled homopolymer chains, the normal modes are referred to as the Rouse modes,[71–73] and the corresponding autocorrelation function is expected to decay exponentially.[71–73] However, in our simulation results, the decay of correlation functions was found to be a stretched exponential due to the presence of various intra- and intermolecular interactions. Such autocorrelation functions were fitted to a stretched exponential function and corresponding mean relaxation time for the respective modes were discerned. We consider the relaxation time corresponding to $N-1$ mode (where N represents the number of beads) to compare with the results extracted from dihedral correlation functions.

6. Ion-pair relaxation times

To probe the structural relaxation of BMIM–PF_6 ion-pairs, we computed the corresponding ion-pair autocorrelation function, $R(t)$. For this purpose, we defined a correlation function $R(t)$ as

$$R(t) = \frac{\langle h(t)h(0)\rangle}{\langle h(0)h(0)\rangle}, \tag{7}$$

where the population variable $h(t)$ is assigned a value unity if an ion-pair which is present at initial $t = 0$ remains intact at time t. In the above equation, the angular brackets represent an ensemble average which includes averaging over all $BMIMPF_6$ ion-pairs as well as all possible time origins. The cutoff distances defining the ion-pairs were identified as 5.5 Å based on the first coordination shell for the distribution of PF_6 and BMIM ions. The ion-pair structural relaxation times $\tau_{\text{BMIM–PF}_6}$ were then estimated as the mean relaxation times obtained by fitting $R(t)$ to a stretched exponential function.

III. RESULTS AND DISCUSSION

A. Coordination between cations, anions, and polymer backbone

The structural aspects of ternary electrolyte systems with different amounts of ionic liquid loadings were investigated by calculating the radial distribution functions (RDFs) and corresponding coordination numbers (CNs) for the lithium-anion and lithium-polymer atomic pairs. Results of RDFs for atomic pairs Li–P and Li–EO at different loadings of IL are presented in Figures 2(a) and 3 respectively for 425 K.

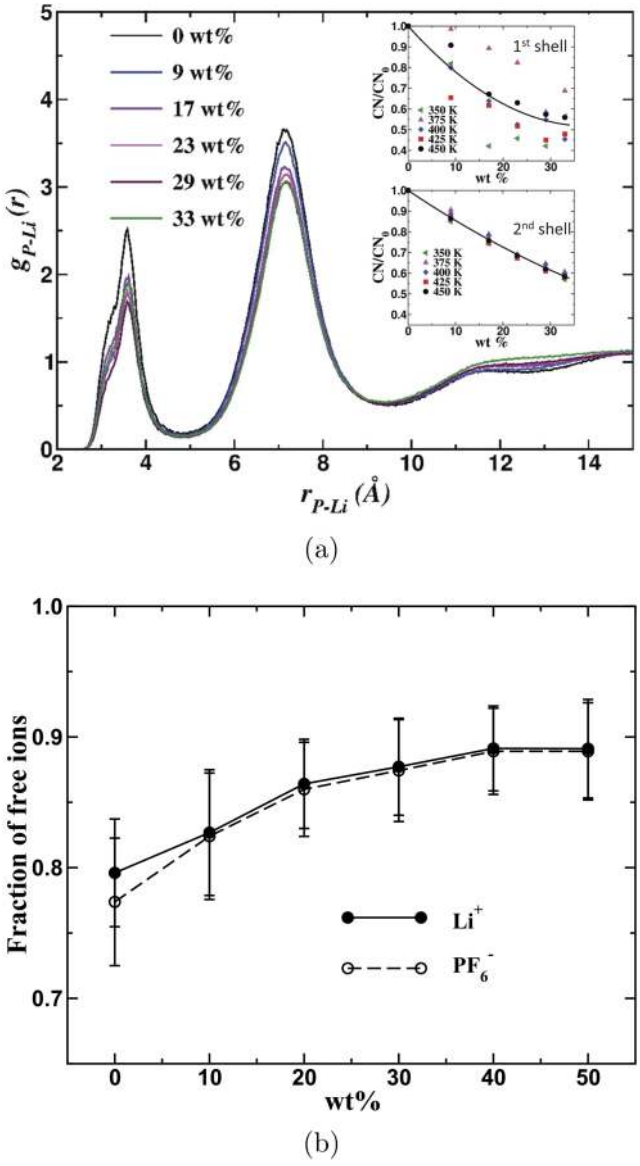

FIG. 2. (a) Radial distribution function of anion-Li ions at various loadings of the IL at 425 K. Coordination number for lithium ions in the first and second coordination shells is shown in insets. (b) Fraction of free Li^+ and PF_6^- ions in ternary electrolyte as a function of the loading of IL at 425 K.

1. Lithium ion coordination with anions

From the results displayed in Figure 2(a), it is seen that the peak of $g_{P–Li}(r)$ in both first and second coordination shells decreases monotonically with the loading of IL, an indication that the addition of IL leads to weaker cation-anion interactions. The coordination numbers of Li^+ ions around P atoms of PF_6^- anion (CN_{Li}) in both coordination shells normalized with those of polymer-salt binary mixture (CN_0) are shown in insets to Figure 2(a). Consistent with the trends seen in $g_{P–Li}(r)$, as the loading of IL increases, a monotonic decrease in CN_{Li} is observed. These results can be understood by noting that the additional $BMIM^+$ and PF_6^- ions supplied by the increased loading of ILs are expected to compete with the coordinated $LiPF_6$ ion-pairs present in the original salt. Such interactions are expected to weaken the Li–PF_6 association affinity and manifest as the observed reduced coordination.

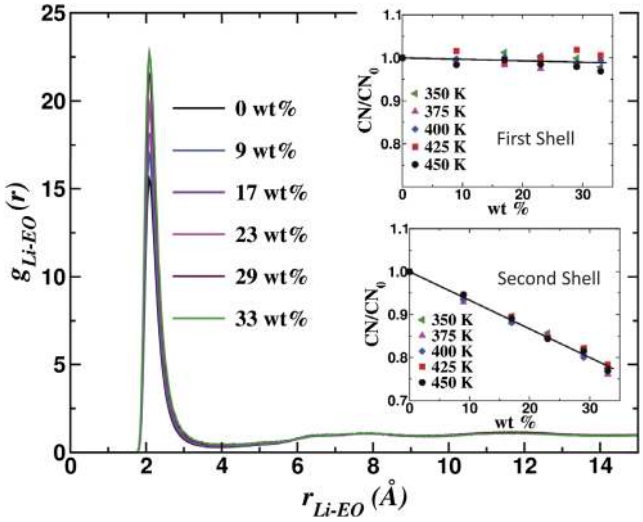

FIG. 3. Radial distribution function of Li–EO atoms at various loadings of the IL. Coordination number for EO atoms in first and second coordination shell are shown as insets.

A direct consequence of the decreased coordination of lithium ions around PF_6^- anions is the enhancement in number of mobile ions in ternary electrolytes as quantified by the fraction of free Li^+ and PF_6^- ions shown in Figure 2(b). A free ion is the one which is not found within the first coordination shell of any of its counterions (a counterion for Li^+ is PF_6^- and vice-versa) in the system. With increasing loading of IL, the PF_6^- ions which are already coordinated to Li^+ ions are expected to be influenced by the ion-ion interactions from the added $BMIM^+$ ions, resulting in increased free Li^+ (and consequently free PF_6^-) ions.

2. Lithium ion coordination with polymer chains

Previous reports in the context of binary polymer-salt electrolytes have demonstrated that the motion of lithium ions in PEO electrolytes is primarily assisted by hopping along the polymer backbone, which in turn is facilitated by the coordination of the Li^+ ions with EO atoms.[74–76] To study the influence of IL on such features, we probed the influence of added IL on the lithium ion association with polymer backbone by calculating $g_{Li^+–EO}(r)$ and CN.

In the results displayed (corresponding to T = 425 K) in Figure 3, at 0 wt. % loading of IL (corresponding to the binary PEO-salt mixture) the location of the first peak in $g_{Li–EO}(r)$ is observed at 2.1 Å, in excellent agreement with earlier reports of atomistic simulations and neutron diffraction experiments.[11,77] More pertinently, the height of peak in $g_{Li–EO}(r)$ is seen to increase with the loading of IL, thereby revealing a stronger association of lithium ions with the polymer backbone. Such results can be rationalized by noting that with the increased loading of IL, there is a weakening of the Li–PF_6 coordination (see Figure 2(a)) which effectively frees up the Li^+ ions to associate more strongly with the EO atoms.

Interestingly however, the number of coordinated EO atoms around Li^+ ions (CN_{EO}) is seen to decrease slightly in the first coordination shell, and a more significant reduction is seen in the second coordination shell with the loading of IL. While on the first sight, $g_{Li–EO}(r)$ and the CN_{EO} results

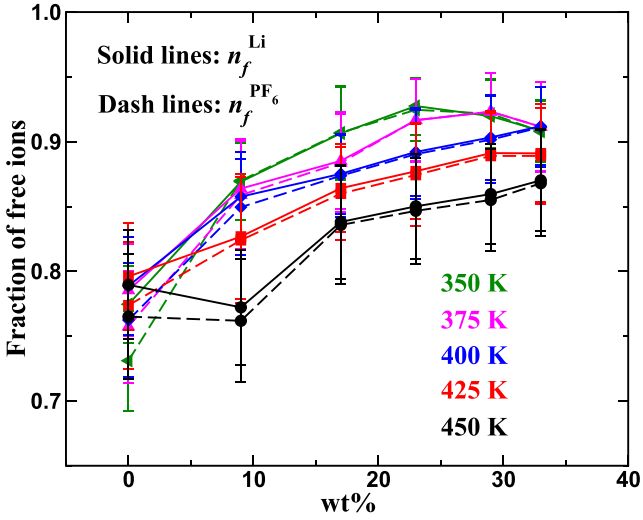

FIG. 4. Fraction of free Li^+ and PF_6^- ions in ternary electrolyte as a function of the loading of IL at different temperatures.

appear to contradict each other, such results can be rationalized by noting that the overall density of lithium ions and EO decreases with the loading of IL (see Table I). Since the CN_{EO} reflects both the density of the system and the $g_{Li-EO}(r)$, the density effects dominate the coordination behavior.

3. Effects of temperature on lithium ion environment

Temperature effects on Li^+ ion environment were probed by calculating the number of free Li^+ and PF_6^- ions at different temperatures. The results, displayed in Figure 4, indicate that the number of free ions *decrease* with increasing temperature. While such results may seem surprising at first sight, they are however consistent with the non-trivial observations reported in earlier simulation studies[78–80] and experiments[81,82] for polymer-salt binary electrolytes. At a physical level, these results can be understood as a consequence of the ion solvation effects of PEO chains. Explicitly, due to the increased thermal motion at higher temperatures, the ion solvation efficiency of PEO and the association of lithium ions with EO atoms are expected to reduce with increase in temperature.[79] The lithium ions which are liberated from polymer backbone can form ion-pairs with anions and manifest as the reduced free ions.

Further insights into the temperature effects on lithium solvation can be drawn through the analysis of clusters between Li^+ and PF_6^- ions and Li^+ and EO atoms (presented in Figure 5). Therein, it is observed that with increase in temperature, the formation of higher order Li–PF_6 clusters is promoted at the expense of lithium ion association with the polymer backbone. Such results are consistent with the physical hypothesis proposed above and serve to rationalize the results presented in Figure 4.

4. BMIM cation-polymer interactions

In Figure 6, we display the results for the coordination between the BMIM cation and the polymer backbone and the influence of simultaneous presence of salt and IL. In the context of a binary mixture of PEO and IL in the absence of salt (indicated as "No $LiPF_6$" in Figure 6), we observe that while there is coordination between the cation and the polymer backbone, the peak intensity is however much weaker relative to the association seen between Li^+ and EO (see Figure 3) and occurs at a farther distance of around 4.0 Å. These results reveal that the BMIM cation polymer interactions, albeit existent, are much weaker relative to the Li^+-polymer interactions.

In ternary mixtures containing both salt and IL and with increasing loading of IL, we observe that there is a decrease in the peak intensity of coordination between BMIM and the polymer backbone. Such a behavior is suggestive of weaker $BMIM^+$–EO interactions and can be rationalized based on the presence of the more preferential cations (Li^+) which compete with $BMIM^+$ ions. In addition, in the presence of $LiPF_6$, the $BMIM^+$ cations have additional PF_6^- anions to interact, which also serves as an additional source of mitigation of the coordination between $BMIM^+$ ions and the backbone.

5. Summary of key findings on ion association behaviors

In summary, analysis of the ion-ion and ion-polymer radial distribution functions in the ternary salt-polymer-IL mixtures leads to the following conclusions: (i) addition of IL promotes a stronger association between the Li^+ ions and the polymer backbone at the expense of Li–PF_6 association; (ii) the temperature dependence of Li–PF_6 coordination behavior is indicative of a larger number of free Li^+ ions at lower temperatures; and (iii) the coordination between $BMIM^+$ ions and the polymer backbone is much weaker relative to the Li^+ cations,

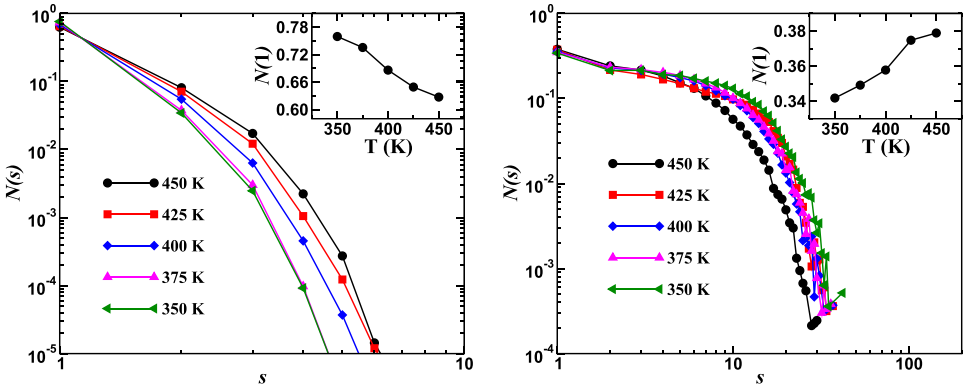

(a)Li-PF_6 clusters (b)Li-EO clusters

FIG. 5. Temperature effects on ion clustering phenomena of (a) Li–PF_6 clusters and (b) Li–EO clusters in ternary polymer-salt-IL electrolytes at 9 wt. % of IL loading. The corresponding total free Li, PF_6 and Li, EO (denoted as $N(1)$) are shown in insets to the figures, respectively.

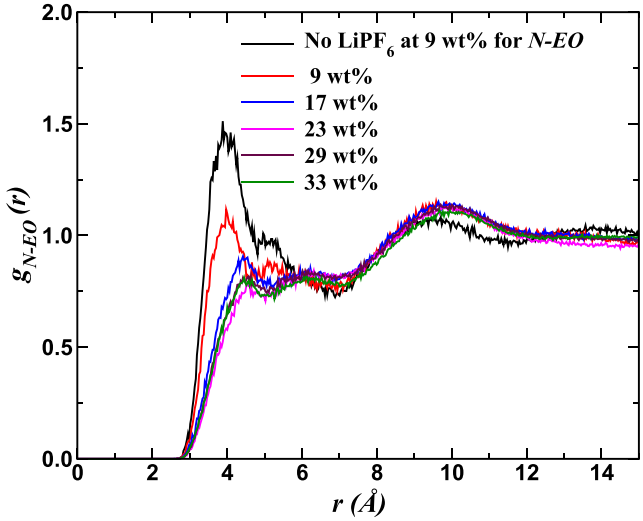

FIG. 6. Radial distribution functions representing weaker BMIM cation-polymer interactions at different loadings of IL into polymer-salt electrolyte.

and becomes more mitigated with an increase in the loading of the IL.

B. Ion mobilities in ternary blend electrolytes

In this section, we report our simulation results for the mobilities of the cations and anions in the ternary blend electrolytes. The mean squared displacements (MSDs) of different ionic species are displayed in Figure 7 for various loadings of the ionic liquid content at $T = 425$ K. Consistent with experimental observations on conductivities, ionic mobilities are seen to be the highest for the *pure* IL and are lower in the salt-free polymer electrolyte (indicated as "9 wt. %, No $LiPF_6$" in the Figure). When $LiPF_6$ salt is additionally present, we observe a further reduction of the ionic MSDs relative to the pure IL mobilities. The MSDs of ionic species are however observed to increase with the loading of $BMIMPF_6$ IL in the polymer-salt electrolyte. The corresponding diffusivity values displayed in Figure 7(b) indicate that the $BMIM^+$ cation displays highest diffusion coefficient in the ternary electrolyte followed by PF_6^- and Li^+ ions. Such results are consistent with the relative trends reported in other studies in the Li^+ doped $PYR_{14}TFSI$ electrolytes.[83–89]

In Figure 8, we display the diffusion coefficient of the individual ionic species as a function of the loading of IL. For Li^+ and PF_6^- ions, we normalize the diffusivities by their values in *IL-free* polymer-salt electrolyte; whereas, for $BMIM^+$ ions, we present diffusivities normalized by their values at the lowest loading of IL probed (9 wt. %). Overall, we observe a monotonic increase of the diffusivities of all the ionic species with the loading of IL. However, the relative increase of the diffusivities is observed to depend on the ionic species. Explicitly, the IL-induced increase of the diffusion coefficients of $BMIM^+$ and PF_6^- ions is seen to be slightly larger compared to the corresponding increase for Li^+ ions.

C. Effect of ILs on polymer segmental dynamics

A number of previous studies have considered binary polymer-salt electrolytes and have established that the motion of ions in such systems is facilitated primarily by the dynamics of polymer segments.[9,58,74,75,90–92] Not surprisingly, in seeking to rationalize the changes in the conductivities arising as a consequence of the introduction of IL in such binary polymer-salt systems, simulations and experiments have implicated the changes in the dynamics of polymer segments as the main mechanism underlying such effects.[5,10–16] As a first step towards unraveling the mechanisms underlying our results for the ionic mobilities, we quantify the changes in the polymer dynamics arising from the introduction of ILs. Towards this objective, the changes in polymer dynamics were characterized by analyzing the relaxation of the correlation function ($C_{\phi\phi}$) of the dihedral angle formed by the backbone C–O–C–C atoms and through normal mode analysis (see Section II C).

In Figure 9(a), we first present a general discussion of the underlying trends by displaying $C_{\phi\phi}$ calculated for *pure* PEO, PEO-9 wt. % IL, polymer-salt, and polymer-salt-IL systems at 425 K. The *pure* PEO is seen to exhibit the fastest polymer dynamics among the different electrolyte systems considered in our simulations. When $LiPF_6$ salt is added (in the absence of IL), a significant slowing of the polymer segmental motion and relaxations are observed. Interestingly, the addition of IL to *pure* PEO is also seen to slow polymer dynamics relative to the *pure* PEO electrolyte. However, the retardation of polymer

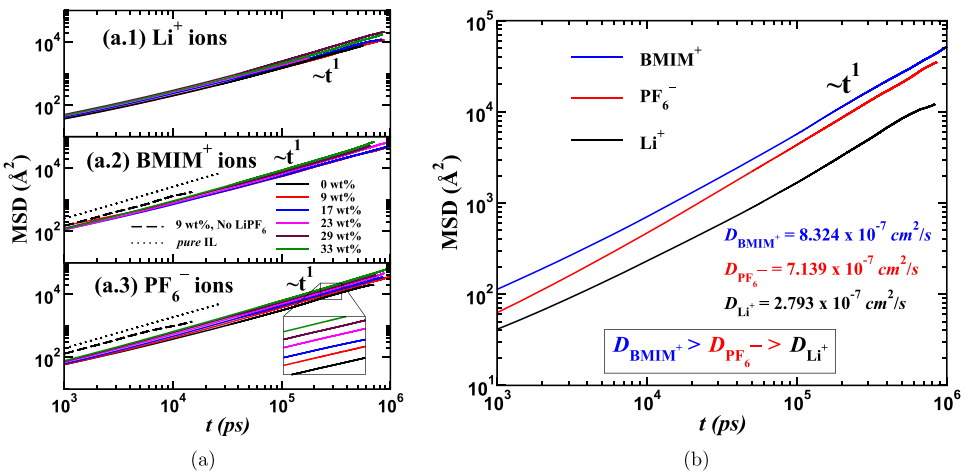

(a) (b)

FIG. 7. Mean squared displacement (MSD) of ions in *pure* IL, polymer-IL and polymer-salt-IL electrolytes for (a.1) Li^+ ions, (a.2) $BMIM^+$ ions, and (a.3) PF_6^- ions at various loadings of the ionic liquid and 425 K. A small portion of the mean-squared displacements is enlarged to display the variations as a function of the loading of the IL. (b) A comparison of the MSDs of all ionic species at a loading of 17 wt. % and 425 K.

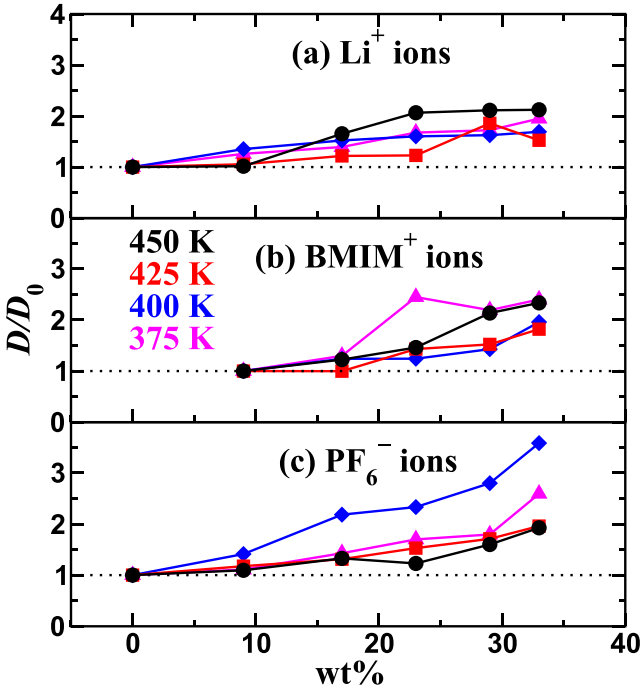

FIG. 8. Normalized diffusion coefficient of ionic species in polymer-salt-IL electrolyte obtained from atomistic simulations for (a) Li^+ ions, (b) $BMIM^+$ ions, and (c) PF_6^- ions as a function of the IL loading at different temperatures.

dynamics due to the IL is seen to be substantially weaker compared to that resulting from $LiPF_6$ salt.

The above results can be understood on the basis of the coordination between the ions and the polymer backbone seen in the results discussed in Section III A. Explicitly, in the context of Figure 3, strong Li^+ ion association with polymer backbone EO atoms was seen. Such a strong coordination can be expected to hinder the mobility of the polymer backbone and reflect in slower polymer relaxations as seen in Figure 9(a).[11,21,75] In the context of the mixture of PEO and IL ("No $LiPF_6$" in Figure 9), we observed that while there is coordination between EO and $BMIM^+$, the peak intensity was much lower and revealed that the BMIM cation polymer interactions were much weaker relative to the Li^+-polymer interactions. Such results rationalize the relatively weak influence of the IL on the polymer relaxations seen in "No $LiPF_6$" systems in Figure 9(a).

In the presence of both salt and IL, three factors come into play: (i) From the results displayed in Figure 6, it is evident that in the presence of IL and salt, there is a decrease of the peak of BMIM cation-polymer coordinations relative to the salt free case. Therein, such results are argued to be a reflection of the stronger competing interactions facilitated by the Li^+–EO pairs; (ii) as was seen in Figure 3, the addition of ILs to the binary salt results in an increase in the peak of the $g(r)$ between Li–EO pairs, which suggests stronger associations between the Li^+ cations and the polymer backbone in ternary blend electrolytes; and (iii) increasing the loading of IL leads to a decrease in the density of Li–EO pairs and an increase in BMIM–EO pairs. From the results displayed in Figure 9(a), it is evident that the polymer relaxation dynamics is seen to be only slightly faster than those seen in binary PEO+$LiPF_6$ systems. These results are suggestive of the fact that the reduced density of Li–EO pairs offset the changes in Li–EO coordination brought about by the IL.

The trends discussed above in the context of $C_{\phi\phi}$ are quantified in Figure 9(b) for the polymer relaxation times τ as a function of the loading of IL. Consistent with our discussion above, it is seen that the polymer relaxation times decrease with increased loading of ILs. Such results are consistent with the previous reports from experiments[14,15] and simulations.[10,11] However, in almost all cases, it is seen that the acceleration in polymer dynamics brought about by the ILs is relatively weak and is less than 15% relative to their values in the IL free case.

Together, the above results indicate that while ILs do act similar to plasticizers and accelerate polymer dynamics in ternary blend electrolytes, the mechanisms underlying are more complex. Indeed, it was seen that the polymer dynamics by itself is slowed by the addition of IL in the absence of the salt. However, the combined effects of reduction in the density of Li^+–EO pairs and the weaker association between $BMIM^+$ ions and EO, are seen to result in faster polymer dynamics in ternary blend mixtures (relative to binary salt-electrolyte systems). Even in such a case, the quantitative influence of ILs is seen to be mitigated in ternary polymer-salt-IL mixtures due to the increased association between the Li and the polymer backbone.

D. Correlation between ion mobilities and polymer segmental dynamics

In this section, we examine the correlations between the IL induced modifications to the ionic mobilities (Figure 8) and

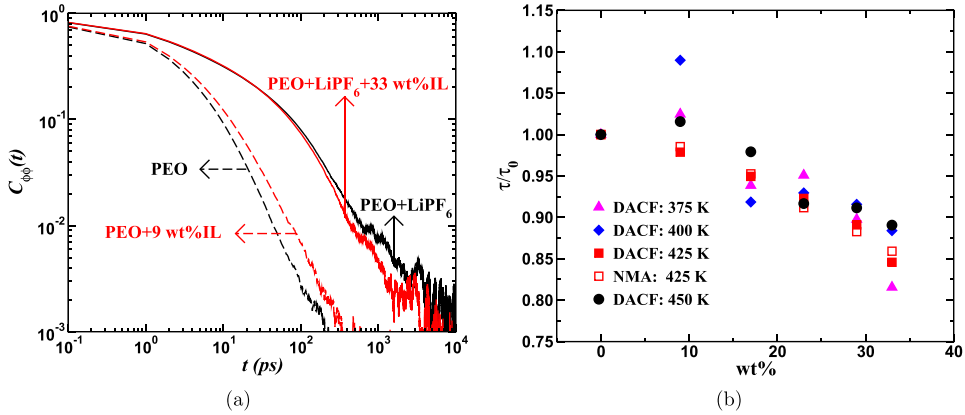

(a) (b)

FIG. 9. (a) Dihedral autocorrelation functions for various polymer electrolytes revealing the role of ionic species in influencing the polymer dynamics. (b) Polymer segmental relaxation time τ in ternary electrolytes with the loading of IL calculated using the dihedral angle (DACF) and normal mode (NMA) correlation functions, where τ_0 is the corresponding value in *IL-free* polymer-salt binary electrolyte.

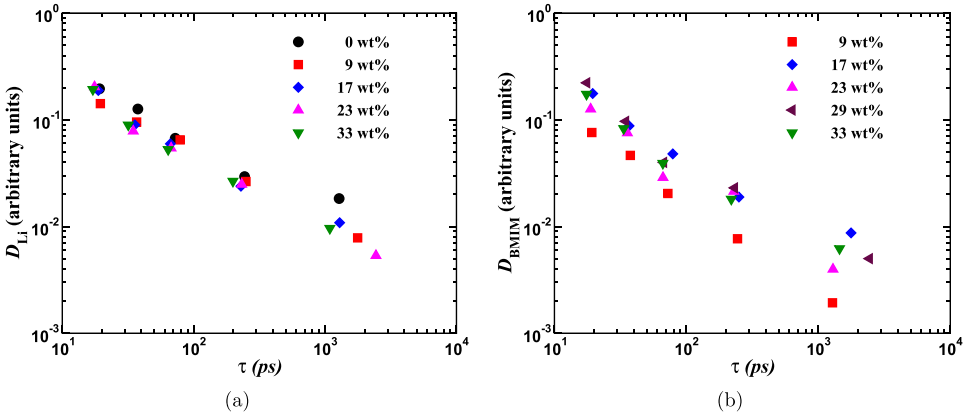

FIG. 10. Diffusion coefficient of (a) Li^+ ions and (b) $BMIM^+$ ions versus polymer segmental relaxation time in ternary electrolytes at different loadings of IL.

the changes in polymer segmental relaxation times presented in Sec. III C. For this purpose, in Figure 10(a) we consider the results for the diffusivities (D_{Li}) at different loadings of ILs and compare their dependence (after shifting by a multiplicative factor to account for the changes in the density of the ion hopping sites) on the polymer relaxation time τ at different temperatures. Such an examination makes no assumptions regarding the dependence of D_{Li} itself on τ, and instead only concerns with the question whether the dependence of D_{Li} on τ remains the same at different loadings of IL. If confirmed, such a result would suggest that the IL-induced changes in the polymer segmental relaxation times constitute the main mechanism underlying the influence of IL on Li^+ ion mobilities.

From the results displayed in Figure 10(a), it is seen that indeed to a good approximation, the ion mobilities at different loadings of ILs fall onto a single universal function of the polymer relaxation times τ. Such results are qualitatively consistent with the findings of Diddens and Heuer[10,11] (albeit, with a different IL and salt combination) who demonstrated that the IL-induced modifications to the polymer motion in-turn influence the dynamics of intra- and interpolymer ion hopping. While they stopped short of examining whether a quantitative correlation can be drawn between τ and the diffusivities, our results in Figure 10(a) confirm such features.

Based on the weak coordination behavior between $BMIM^+$ and EO units, the motion of $BMIM^+$ ions is expected to be less sensitive to the polymer dynamics. In Figure 10(b), we display a comparison between D and τ for the $BMIM^+$ ions in a framework similar to the one depicted for Li^+ ions. While the results for $BMIM^+$ ions appear qualitatively similar to those depicted in Figure 10(a), there is evidently more scatter in Figure 10(b) reflecting the weaker correlation between the changes in IL-induced $BMIM^+$ ion mobilities and the corresponding modifications to the polymer relaxation times.

Other studies[93–96] have suggested that the motion of ion-pairs in such IL based systems is sensitive to the ion-pair relaxation dynamics. Motivated by such findings, in our work we determined the BMIM–PF_6 structural relaxation times using ion-pair correlation function, $R(t)$, as discussed in Section II C at different temperatures and IL loadings and display the corresponding results in Figure 11(a). It is seen that increasing the loading of IL leads to a decrease in the relaxation times, a trend which is consistent with the faster dynamics of ion hopping that is likely to occur when there are more such ion-pairs present in the system. Moreover, in contrast to polymer relaxation times wherein different competing mechanisms mitigated the effects of ILs, the changes observed in $\tau_{BMIM-PF_6}$ are seen to be considerably more significant.

In Figure 11(b) we depict a comparison between the diffusivities of $BMIM^+$ ions and the corresponding $\tau_{BMIM-PF_6}$. Therein, a near perfect correlation is observed, suggesting that the diffusivities of the IL cations are strongly slaved to cation-anion ion-pair relaxation times. Together, such results suggest that the influence of IL on $BMIM^+$ ion mobilities can be rationalized as a consequence of the modulation of the ion-pair relaxation times $\tau_{BMIM-PF_6}$. Moreover, since the changes in $\tau_{BMIM-PF_6}$ are found to be relatively larger in magnitude compared to the polymer relaxation times, the increase in the mobilities of the ions of IL are also more significant compared to that of Li^+ ions.

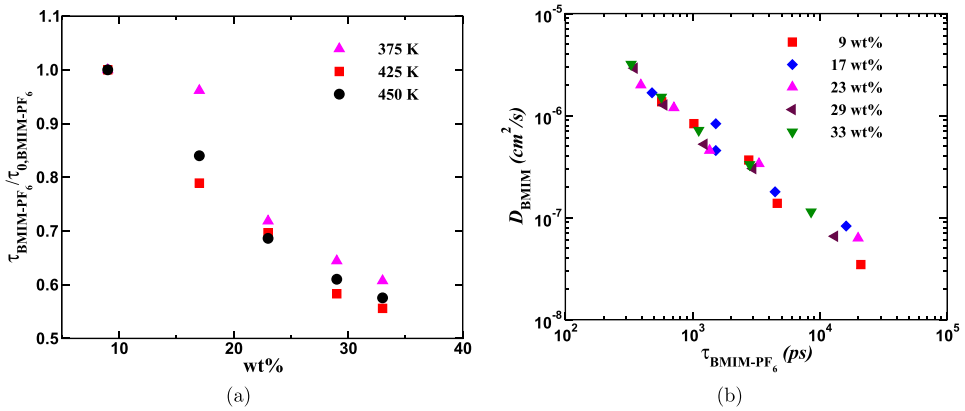

FIG. 11. (a) BMIM–PF_6 ion-pair structural relaxation time calculated using ion-pair correlation function, $R(t)$ as a function of the loading of IL at different temperatures and (b) diffusion coefficient of $BMIM^+$ ions versus ion-pair relaxation time in ternary electrolytes at different loadings of IL.

Together, the results presented in this section provide an understanding of the mechanisms underlying the ion mobilities presented in Section III B. Our results suggest that to a good approximation, the IL-induced changes in the diffusivities of Li^+ ions arise primarily from the changes in the polymer segmental dynamics. Since the modulations in the latter were mitigated due to competing interactions, the corresponding changes in Li^+ ion mobilities were also only modest (Figure 8). In contrast, the mobilities of $BMIM^+$ ions were found to be more strongly tied to the ion-pair relaxations. Since the latter displays more significant changes with the introduction of ILs, correspondingly the cations and anions of the ILs displayed a stronger dependence on the loading of IL. Moreover, since the ionic mobilities are correlated to distinct time scales, such findings may help design polymer electrolyte membranes which possess high ionic conductivities without the concomitant reduction in mechanical strength.

IV. CONCLUDING REMARKS

To summarize, we used atomistic simulations to study the mechanisms underlying the structure and ion transport in ternary polymer electrolytes containing PEO–$LiPF_6$ and $BMIMPF_6$ ionic liquids. Our study considered the effects of both the loading of IL and temperature and presented results on the radial distribution functions, coordination numbers, polymer segmental relaxation, and ion-pair relaxation times.

Our results revealed that the addition of IL enhances the association of Li^+ ions with the polymer backbone and weakens the coordination between Li^+ and PF_6^- ions. As a consequence the fraction of free Li^+ ions were seen to increase with loading of IL. At lower temperatures, the fraction of free Li^+ ions were found to be enhanced to a larger extent relative to the case of binary PEO-salt mixture. Such results provide a qualitative rationalization of the more significant changes in conductivity seen from adding ILs at lower temperatures.

An interesting outcome of our study was the demonstration that $BMIM^+$ ions do not act as a plasticizer to the pure polymer electrolyte. Instead, due to the weak coordination between $BMIM^+$ ions and the polymer backbone, the polymer relaxation behavior in salt-free electrolyte was observed to be slowed with the addition of IL. In the ternary polymer electrolyte, the polymer relaxations were observed to be accelerated relative to polymer-salt mixture. However, due to the competing effects of the weaker coordination between IL and polymer backbone, reduction in density of ion-pairs, and the increased association of Li^+ ions with the polymer backbone, the overall changes in the polymer relaxation times were observed to be mitigated.

Our results indicated that the ionic mobilities increase with the loading of IL. However, the relative enhancements in the mobilities of PF_6^- and $BMIM^+$ ions were found to be more significant compared to Li^+ ions. Examination of the relation between the diffusivities and the various relaxation times suggested that Li^+ ion diffusivities were strongly correlated to polymer dynamics, and the $BMIM^+$ diffusivities are less sensitive to such time scales and were found to be more strongly correlated to the relaxation dynamics of BMIM–PF_6 ion-pairs. These results suggest that distinct mechanisms underlie the ion mobilities in such ternary blend polymer electrolytes and can potentially pave the way for optimization of the conductivity characteristics of such mixtures.

SUPPLEMENTARY MATERIAL

See supplementary material for comparison of the differences between the full charge model and charge scaled model employed in our simulations.

ACKNOWLEDGMENTS

We thank Professor Acevedo for clarifications regarding the intra-atomic force field parameters for the ionic liquid. The authors acknowledge the Texas Advanced Computing Center (TACC) at The University of Texas at Austin for providing computing resources that have contributed to the research results reported within this paper. This work was supported in part by grants from the Robert A. Welch Foundation (Grant No. F1599), the National Science Foundation (Grant No. DMR-1306844), and the U.S. Army Research Office under Grant No. W911NF-13-1-0396.

[1] M. Armand, F. Endres, D. R. MacFarlane, H. Ohno, and B. Scrosati, Nat. Mater. **8**, 621 (2009).
[2] N. V. Plechkova and K. R. Seddon, Chem. Soc. Rev. **37**, 123 (2008).
[3] Y.-S. Ye, J. Rick, and B.-J. Hwang, J. Mater. Chem. A **1**, 2719 (2013).
[4] H. Ohno, Electrochim. Acta **46**, 1407 (2001).
[5] J. Shin, W. Henderson, and S. Passerini, J. Electrochem. Soc. **152**, A978 (2005).
[6] H. Olivier-Bourbigou and L. Magna, J. Mol. Catal. A: Chem. **182**, 419 (2002).
[7] J. C. Araque, S. K. Yadav, M. Shadeck, M. Maroncelli, and C. J. Margulis, J. Phys. Chem. B **119**, 7015 (2015).
[8] J. C. Araque, J. J. Hettige, and C. J. Margulis, J. Phys. Chem. B **119**, 12727 (2015).
[9] S. Mogurampelly, O. Borodin, and V. Ganesan, Annu. Rev. Chem. Biomol. Eng. **7**, 349 (2016).
[10] D. Diddens and A. Heuer, ACS Macro Lett. **2**, 322 (2013).
[11] D. Diddens and A. Heuer, J. Phys. Chem. B **118**, 1113 (2014).
[12] J. Shin, W. Henderson, S. Scaccia, P. Prosini, and S. Passerini, J. Power Sources **156**, 560 (2006).
[13] J.-W. Choi, G. Cheruvally, Y.-H. Kim, J.-K. Kim, J. Manuel, P. Raghavan, J.-H. Ahn, K.-W. Kim, H.-J. Ahn, D. S. Choi, and C. E. Song, Solid State Ionics **178**, 1235 (2007).
[14] M. Joost, M. Kunze, S. Jeong, M. Schoenhoff, M. Winter, and S. Passerini, Electrochim. Acta **86**, 330 (2012).
[15] S. K. Chaurasia, A. L. Saroj, Shalu, V. K. Singh, A. K. Tripathi, A. K. Gupta, Y. L. Verma, and R. K. Singh, AIP Adv. **5**, 077178 (2015).
[16] L. T. Costa, R. L. Lavall, R. S. Borges, J. Rieumont, G. G. Silva, and M. C. C. Ribeiro, Electrochim. Acta **53**, 1568 (2007).
[17] Z. Li, J. Jiang, G. Lei, and D. Gao, Polym. Adv. Technol. **17**, 604 (2006).
[18] J. Mondal, E. Choi, and A. Yethiraj, Macromolecules **47**, 438 (2014).
[19] S. Raju, K. S. Hariharan, D.-H. Park, H. Kang, and S. M. Kolake, J. Power Sources **293**, 983 (2015).
[20] L. Costa and M. Ribeiro, J. Chem. Phys. **124**, 184902 (2006).
[21] L. T. Costa and M. C. C. Ribeiro, J. Chem. Phys. **127**, 164901 (2007).
[22] L. T. Costa, B. Sun, F. Jeschull, and D. Brandell, J. Chem. Phys. **143**, 024904 (2015).
[23] W. Jorgensen, D. Maxwell, and J. TiradoRives, J. Am. Chem. Soc. **118**, 11225 (1996).
[24] S. V. Sambasivarao and O. Acevedo, J. Chem. Theory Comput. **5**, 1038 (2009).
[25] J. Lopes, J. Deschamps, and A. Padua, J. Phys. Chem. B **108**, 2038 (2004).
[26] F. Dommert, K. Wendler, R. Berger, L. Delle Site, and C. Holm, ChemPhysChem **13**, 1625 (2012).
[27] O. Borodin, J. Phys. Chem. B **113**, 11463 (2009).
[28] O. Borodin, G. D. Smith, and W. Henderson, J. Phys. Chem. B **110**, 16879 (2006).

[29]O. Borodin, W. Gorecki, G. D. Smith, and M. Armand, J. Phys. Chem. B **114**, 6786 (2010).
[30]C. Y. Son, J. G. McDaniel, J. R. Schmidt, Q. Cui, and A. Yethiraj, J. Phys. Chem. B **120**, 3560 (2016).
[31]J. G. McDaniel, E. Choi, C. Y. Son, J. R. Schmidt, and A. Yethiraj, J. Phys. Chem. B **120**, 231 (2016).
[32]T. Morrow and E. Maginn, J. Phys. Chem. B **106**, 12807 (2002).
[33]V. Chaban, Phys. Chem. Chem. Phys. **13**, 16055 (2011).
[34]V. V. Chaban, I. V. Voroshylova, and O. N. Kalugin, Phys. Chem. Chem. Phys. **13**, 7910 (2011).
[35]B. L. Bhargava and S. Balasubramanian, J. Chem. Phys. **127**, 114510 (2007).
[36]T. G. A. Youngs and C. Hardacre, ChemPhysChem **9**, 1548 (2008).
[37]Y. Zhang and E. J. Maginn, J. Phys. Chem. B **116**, 10036 (2012).
[38]Y. Zhang, L. Xue, F. Khabaz, R. Doerfler, E. L. Quitevis, R. Khare, and E. J. Maginn, J. Phys. Chem. B **119**, 14934 (2015).
[39]C. Cadena, J. Anthony, J. Shah, T. Morrow, J. Brennecke, and E. Maginn, J. Am. Chem. Soc. **126**, 5300 (2004).
[40]F. Müller-Plathe and W. F. van Gunsteren, J. Chem. Phys. **103**, 4745 (1995).
[41]N. Sieffert and G. Wipff, J. Phys. Chem. B **110**, 13076 (2006).
[42]G. Chevrot, R. Schurhammer, and G. Wipff, Phys. Chem. Chem. Phys. **8**, 4166 (2006).
[43]A. Mondal and S. Balasubramanian, J. Phys. Chem. B **118**, 3409 (2014).
[44]A. P. Sunda, A. Monda, and S. Balasubramanian, Phys. Chem. Chem. Phys. **17**, 4625 (2015).
[45]K. G. Sprenger, V. W. Jaeger, and J. Pfaendtner, J. Phys. Chem. B **119**, 5882 (2015).
[46]W. Kohn and L. Sham, Phys. Rev. **140**, 1133 (1965).
[47]P. Hohenberg and W. Kohn, Phys. Rev. B **136**, B864 (1964).
[48]A. D. Becke, J. Chem. Phys. **98**, 5648 (1993).
[49]C. Lee, W. Yang, and R. Parr, Phys. Rev. B **37**, 785 (1988).
[50]L. Martinez, R. Andrade, E. G. Birgin, and J. M. Martinez, J. Comput. Chem. **30**, 2157 (2009).
[51]S. Mogurampelly and V. Ganesan, Macromolecules **48**, 2773 (2015).
[52]S. Mogurampelly and V. Ganesan, Solid State Ionics **286**, 57 (2016).
[53]S. Plimpton, J. Comput. Phys. **117**, 1 (1995).
[54]S. Neyertz and D. Brown, Macromolecules **43**, 9210 (2010).
[55]A. B. Bortz, M. H. Kalos, and J. L. Lebowitz, J. Comput. Phys. **17**, 10 (1975).
[56]S. Mogurampelly, V. Sethuraman, V. Pryamitsyn, and V. Ganesan, J. Chem. Phys. **144**, 154905 (2016).
[57]B. Hanson, V. Pryamitsyn, and V. Ganesan, J. Phys. Chem. B **116**, 95 (2012).
[58]B. Hanson, V. Pryamitsyn, and V. Ganesan, ACS Macro Lett. **2**, 1001 (2013).
[59]J. Lopes and A. Padua, J. Phys. Chem. B **110**, 3330 (2006).
[60]J. Dupont, J. Braz. Chem. Soc. **15**, 341 (2004).
[61]W. Jiang, Y. Wang, and G. A. Voth, J. Phys. Chem. B **111**, 4812 (2007).
[62]J. Wang and H. Wang, *Structures and Interactions of Ionic Liquids* (Springer-Verlag, 2014), Vol. 151, pp. 39–77.
[63]E. Sevick, P. Monson, and J. Ottino, J. Chem. Phys. **88**, 1198 (1988).
[64]S. Salaniwal, S. Cui, H. Cochran, and P. Cummings, Langmuir **17**, 1784 (2001).
[65]P. D. Godfrin, R. Castaneda-Priego, Y. Liu, and N. J. Wagner, J. Chem. Phys. **139**, 154904 (2013).
[66]G. Pandav, V. Pryamitsyn, and V. Ganesan, Langmuir **31**, 12328 (2015).
[67]G. Pandav, V. Pryamitsyn, J. Errington, and V. Ganesan, J. Phys. Chem. B **119**, 14536 (2015).
[68]O. Borodin, G. D. Smith, R. Bandyopadhyaya, and E. Byutner, Macromolecules **36**, 7873 (2003).
[69]T. V. M. Ndoro, M. C. Boehm, and F. Müller-Plathe, Macromolecules **45**, 171 (2012).
[70]V. Pryamitsyn and V. Ganesan, Macromolecules **39**, 844 (2006).
[71]P. E. Rouse, J. Chem. Phys. **21**, 1272 (1953).
[72]M. Doi and S. F. Edwards, *The Theory of Polymer Dynamics*, International Series of Monographs on Physics (Oxford University Press, New York, 1988).
[73]K. Kremer and G. Grest, J. Chem. Phys. **92**, 5057 (1990).
[74]O. Borodin and G. D. Smith, Macromolecules **39**, 1620 (2006).
[75]A. Maitra and A. Heuer, Phys. Rev. Lett. **98**, 227802 (2007).
[76]D. T. Hallinan, Jr. and N. P. Balsara, Annu. Rev. Mater. Res. **43**, 503 (2013).
[77]G. Mao, M. Saboungi, D. Price, M. Armand, and W. Howells, Phys. Rev. Lett. **84**, 5536 (2000).
[78]M. Ratner and A. Nitzan, Faraday Discuss. **88**, 19 (1989).
[79]V. Payne, M. Forsyth, M. Ratner, D. Shriver, and S. Deleeuw, J. Chem. Phys. **100**, 5201 (1994).
[80]K.-J. Lin and J. K. Maranas, Macromolecules **45**, 6230 (2012).
[81]M. Kakihana, S. Schantz, and L. Torell, J. Chem. Phys. **92**, 6271 (1990).
[82]W. Wang, G. J. Tudryn, R. H. Colby, and K. I. Winey, J. Am. Chem. Soc. **133**, 10826 (2011).
[83]M. Gouverneur, J. Kopp, L. van Wuellen, and M. Schoenhoff, Phys. Chem. Chem. Phys. **17**, 30680 (2015).
[84]D. H. C. Wong, J. L. Thelen, Y. Fu, D. Devaux, A. A. Pandya, V. S. Battaglia, N. P. Balsara, and J. M. DeSimone, Proc. Natl. Acad. Sci. U. S. A. **111**, 3327 (2014).
[85]H. Tokuda, S. Tsuzuki, M. A. B. H. Susan, K. Hayamizu, and M. Watanabe, J. Phys. Chem. B **110**, 19593 (2006).
[86]C. J. F. Solano, S. Jeremias, E. Paillard, D. Beljonne, and R. Lazzaroni, J. Chem. Phys. **139**, 034502 (2013).
[87]J. B. Haskins, W. R. Bennett, J. J. Wu, D. M. Hernandez, O. Borodin, J. D. Monk, C. W. Bauschlicher, Jr., and J. W. Lawson, J. Phys. Chem. B **118**, 11295 (2014).
[88]J. B. Haskins, C. W. Bauschlicher, Jr., and J. W. Lawson, J. Phys. Chem. B **119**, 14705 (2015).
[89]F. Castiglione, E. Ragg, A. Mele, G. B. Appetecchi, M. Montanino, and S. Passerini, J. Phys. Chem. Lett. **2**, 153 (2011).
[90]C. Berthier, W. Gorecki, M. Minier, M. B. Armand, J. M. Chabagno, and P. Rigaud, Solid State Ionics **11**, 91 (1983).
[91]M. A. Ratner and D. F. Shriver, Chem. Rev. **88**, 109 (1988).
[92]D. Diddens, A. Heuer, and O. Borodin, Macromolecules **43**, 2028 (2010).
[93]J. R. Sangoro, C. Iacob, A. L. Agapov, Y. Wang, S. Berdzinski, H. Rexhausen, V. Strehmel, C. Friedrich, A. P. Sokolov, and F. Kremer, Soft Matter **10**, 3536 (2014).
[94]K. Nakamura, T. Saiwaki, and K. Fukao, Macromolecules **43**, 6092 (2010).
[95]K. Nakamura, T. Saiwaki, K. Fukao, and T. Inoue, Macromolecules **44**, 7719 (2011).
[96]K. Nakamura, K. Fukao, and T. Inoue, Macromolecules **45**, 3850 (2012).